

A versatile source to produce high-intensity, pulsed supersonic radical beams for crossed-beam experiments: The cyanogen radical $\text{CN}(X^2\Sigma^+)$ as a case study

R. I. Kaiser,^{a)} J. W. Ting, L. C. L. Huang, N. Balucani,^{b)} O. Asvany,^{c)} and Y. T. Lee
Institute of Atomic and Molecular Sciences, 1, Section 4, Roosevelt Rd. 107 Taipei, Taiwan, Republic of China

H. Chan, D. Stranges, and D. Gee
Department of Chemistry, University of California, Berkeley, Berkeley, California 94720

(Received 27 April 1999; accepted for publication 25 June 1999)

In our laboratory a novel and convenient technique has been developed to generate an intense pulsed cyano radical beam to be employed in crossed molecular beam experiments investigating the chemical dynamics of bimolecular reactions. CN radicals in their ground electronic state $^2\Sigma^+$ are produced *in situ* via laser ablation of a graphite rod at 266 nm and 30 mJ output power and subsequent reaction of the ablated species with molecular nitrogen, which acts also as a seeding gas. A chopper wheel located after the ablation source and before the collision center selects a $9\ \mu\text{s}$ segment of the beam. By changing the delay time between the pulsed valve and the chopper wheel, we can select a section of the pulsed $\text{CN}(X^2\Sigma^+)$ beam choosing different velocities in the range of $900\text{--}1920\ \text{ms}^{-1}$ with speed ratios from 4 to 8. A high-stability analog oscillator drives the motor of the chopper wheel (deviations less than 100 ppm of the period), and a high-precision reversible motor driver is interfaced to the rotating carbon rod. Both units are essential to ensure a stable cyanogen radical beam with velocity fluctuations of less than 3%. The high intensity of the pulsed supersonic CN beam of about $2\text{--}3 \times 10^{11}\ \text{cm}^{-3}$ is three orders of magnitude higher than supersonic cyano radical beams employed in previous crossed molecular beams experiments. This data together with the tunable velocity range clearly demonstrate the unique power of our newly developed *in situ* production of a supersonic CN radical beam. This versatile concept is extendible to generate other intense, pulsed supersonic beams of highly unstable diatomic radicals, among them BC, BN, BO, BS, CS, SiC, SiN, SiO, and SiS, which are expected to play a crucial role in interstellar chemistry, chemistry in the solar system, and/or combustion processes. © 1999 American Institute of Physics. [S0034-6748(99)04911-4]

I. INTRODUCTION

The detailed chemical reaction dynamics of ground-state cyano radicals $\text{CN}(X^2\Sigma^+)$ are of fundamental importance in various terrestrial and extraterrestrial environments. Initiated by the solar photolyses of hydrogen cyanide (HCN) and cyanogen (C_2N_2) in the atmospheres of the outer planets and satellites of our solar system such as Jupiter, Saturn, Titan, Uranus, and possibly Neptune,¹⁻³ $\text{CN}(X^2\Sigma^+)$ radicals are strongly considered to synthesize unsaturated nitriles such as cyanoacetylene (HCCCN), vinylcyanide ($\text{C}_2\text{H}_3\text{CN}$), together with more complex nitriles. Likewise, these reactions might lead to highly unsaturated cyanopolyynes [$\text{H}-(\text{C}\equiv\text{C})_n-\text{CN}$ ($n=1\text{--}5$)], which were observed in various molecular clouds in the interstellar medium such as TMC-1,⁴ and the outflow of the carbon star IRC+10216.⁵ Besides these more

“exotic” environments, the critical role of CN in combustion processes in fuel-rich flames and coal combustion has been recognized.⁶

Due to the importance of these CN reactions, a multitude of temperature-dependent rate constants were studied employing the pulsed-laser photolyses/laser-induced fluorescence (LP/LIF) method under bulk conditions.⁷ Recent laboratory measurements at temperatures as low as 13 K utilized low temperature techniques.⁸ These studies made use of photolyzing CN-containing precursors such as NOCN, C_2N_2 , XCN (X=Cl,Br,I) or generating CN radicals in a low-pressure fast-flow chemical reactor. Although valuable kinetic data are obtained by monitoring the decay kinetics of the CN radical, these investigations could not provide reaction products, information on the involved potential-energy surfaces, or the chemical dynamics on the elementary reaction steps. Therefore, additional studies are clearly necessary to address these open questions.

The crossed molecular beams technique^{9,10} represents a versatile and excellent tool to unravel these chemical reaction dynamics, triply differential cross sections, and reaction products of $\text{CN}(X^2\Sigma^+)$ reactions. These experiments are performed under well-characterized primary and secondary

^{a)}Also at the Department of Physics, Technical University Chemnitz–Zwickau, 09107 Chemnitz, Germany. Corresponding author; electronic mail: kaiser@po.iams.sinica.edu.tw

^{b)}Present address: University of Perugia, Dipartimento di Chimica, 06123 Perugia, Italy.

^{c)}Also at the Department of Physics, Technical University Chemnitz–Zwickau, 09107 Chemnitz, Germany.

TABLE I. Typical velocities and speed ratios of different parts of the pulsed $\text{CN}(X^2\Sigma^+)$ beam.

Seeding gas	Velocity (ms^{-1})	Speed ratio
N_2	900	8.5–8.0
N_2	1185	6.5–7.0
N_2	1320	5.4–6.0
N_2	1396	6.0–6.5
N_2	1560	6.3–7.3
N_2	1720	5.0–5.4
N_2	1920	4.0–4.5

beam conditions with narrow velocity distributions, well-defined interaction angle, and hence, a well-known collision energy. Most important, these experiments are performed under single collision conditions. This means that in a binary reaction $A + BC \rightarrow [ABC]^* \rightarrow AB + C$, one species A reacts only with one species BC without collisional stabilization or successive reaction of the initially formed $[ABC]^*$ complex (exclusion of three-body reactions). This requirement guarantees that the nascent reaction product undergoes no secondary reaction and no collision-induced depopulation of the rotational, vibrational, and electronic states of the products. So far, the investigations on important CN radical reactions have been elucidated only for two tetra atomic systems, $\text{CN} + \text{D}_2$ (Ref. 11) and $\text{CN} + \text{O}_2$,¹² employing the crossed molecular beams approach. For the $\text{CN} + \text{D}_2$ reaction, the experiments and quasiclassical trajectory (QCT) calculations on an accurate potential-energy surface indicated that CN abstracts a hydrogen atom in a direct reaction. In these studies, a 5% cyanogen, C_2N_2 , beam seeded in hydrogen, H_2 , was photolyzed at 193 nm to yield about 10^8 CN radicals cm^{-3} in the interaction regions of the crossed molecular beams apparatus.¹³ The D atom was detected by (1+1) resonance-enhanced multiphoton ionization (REMPI). A variant of the three-dimensional imaging technique, i.e., the Doppler-selected time-of-flight (TOF) technique, was employed to map out the three-dimensional center-of-mass flux distribution. We wish to recall, however, that even if this $\text{CN} + \text{D}_2$ system may be regarded as a prototype for CN reactions because of its simplicity, the reaction mechanism with more complex molecules such as unsaturated hydrocarbons and the formation of unsaturated nitriles is expected to be different with the addition of CN to the π bond being dominant.

But, what experimental detection scheme in crossed molecular beam experiments of CN with unsaturated hydrocarbons is suitable to investigate these gas-phase reactions? Most important, highly unstable and reactive products with often unknown spectroscopic properties have to be probed. Hence, the majority of interesting interstellar/combustion radicals such as long-chain nitriles and cummulenes cannot be sampled via optical detection schemes such as laser-induced fluorescence and resonance-enhanced multiphoton ionization. If D atoms are released, they could be probed via a 1+1 REMPI as performed in the $\text{CN} + \text{D}_2$ reaction. Although this powerful technique has almost zero background, often very expensive (per)deuterated precursor molecules are required to do crossed beam reactions of CN radicals with,

for example, unsaturated hydrocarbons. Therefore, a ‘‘universal’’ detector such as an electron-impact ionizer coupled to a quadrupole mass spectrometer is desirable. However, the number density of 10^8 CN radicals cm^{-3} of currently operating CN sources is about two orders of magnitudes too low to be employed in these experiments: here, previous crossed-beam studies of CN radicals generated via photodissociation of helium-seeded C_2N_2 , BrCN, or ICN at 193 nm did not yield any reactive scattering signal with acetylene, C_2H_2 , or ethylene, C_2H_4 .¹⁴ Hence, an alternative CN production method is imperative, and the new supersonic CN source should (a) give number densities of at least 10^{10} CN radicals cm^{-3} in the interaction region, (b) minimize other CN-containing clusters, (c) tune the velocity of the CN beam to investigate the chemical dynamics at different collision energies, and (d) generate a highly reproducible and long-term stable supersonic beam.

This contribution is organized as follows: Sec. II describes the experimental setup of the supersonic CN source and the CN beam generation. The results on velocities, speed ratios, and long-term stability of the supersonic CN beam, beam composition, and number densities in the interaction region are given in Sec. III. Finally, the discussion in Sec. IV centers on specified demands and investigates the possibility to employ our newly developed source to generate other highly reactive diatomic intermediates/radicals.

II. EXPERIMENTAL SETUP

A. Design of the $\text{CN}(X^2\Sigma^+)$ source, incorporation in the crossed-beam machine, and beam generation

The CN radical in its ground electronic state $^2\Sigma^+$ is produced *in situ* via laser ablation of a graphite rod and subsequent reaction of the ablated species with molecular nitrogen which acts also as the seeding gas. The center of the CN source is made of an aluminum block interfaced to a stainless-steel/brass frame. The graphite rod is located 0.05 mm inside the extension channel of a Proch–Trickl pulsed valve¹⁵ with a 1.0 mm nozzle diameter. The extension channel goes 7 mm from the pulsed valve to the laser ablation region and intersects the laser channel at 90°. The graphite rod is attached to a motor which and is kept in a helical motion during the laser irradiation. The rotational direction of the carbon rod is reversed by changing the polarities of the motor via an automated voltage switcher box located outside the vacuum, c.f. Sec. II B. To produce a $\text{CN}(X^2\Sigma^+)$ beam, the 266 nm and 30 Hz output of a Spectra Physics GCR-270-30 Nd:YAG laser is focused with 30 mJ per pulse on the carbon rod to a spot less than 0.4 mm diam. If a laser output larger than 30 mJ per pulse is applied, excited CN radicals are formed, cf. Sec. III D. The laser beam entrance channel is completely isolated from the second source region to avoid reaction of CN radicals in the first source with background reactant molecules and differentially pumped by an oil-free 150 s^{-1} turbomolecular pump backed by a membrane pump. The pulsed valve operates at 60 Hz, 80 μs pulses, and 4 atm backing pressure of neat nitrogen and is driven by -600 V pulses. The laser-ablated species react with the ni-

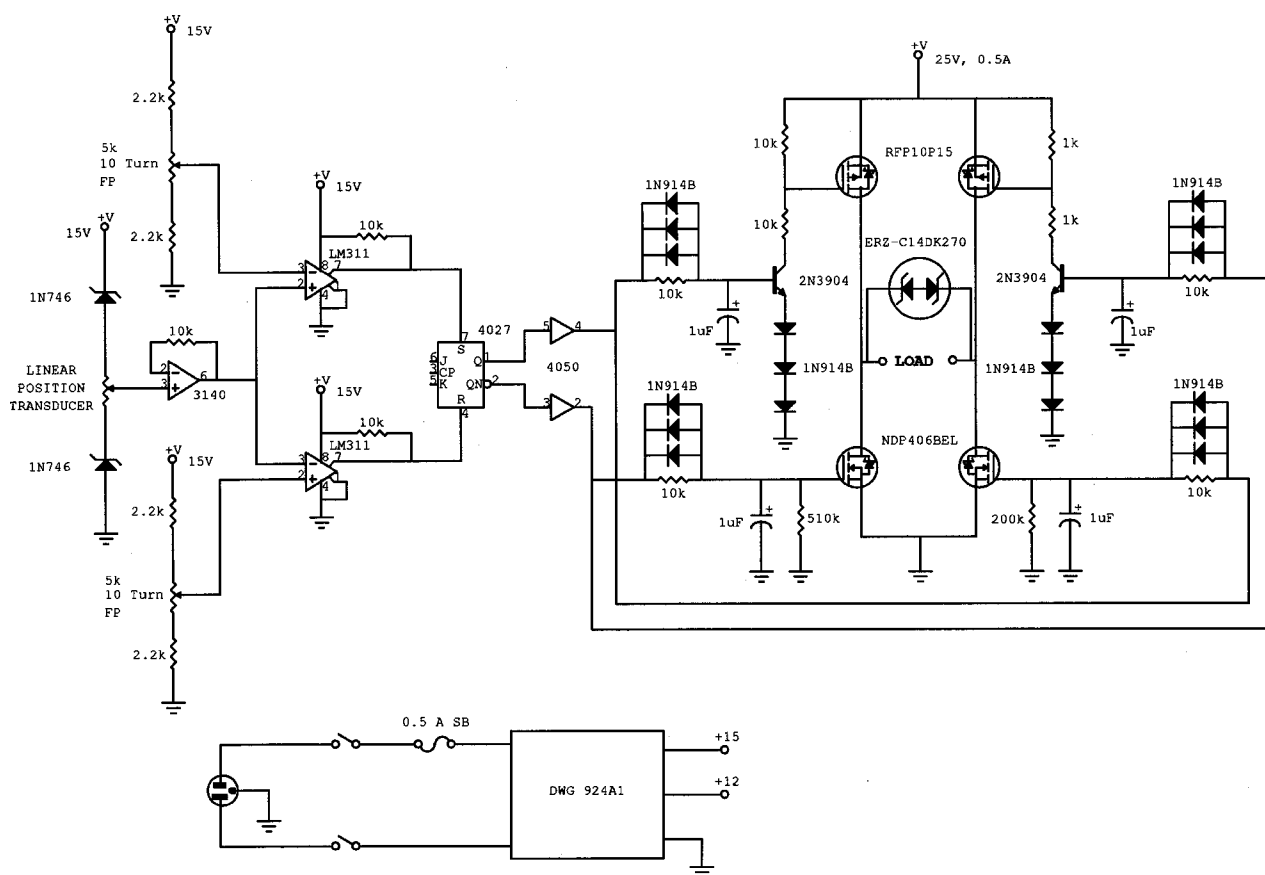


FIG. 1. Circuit diagram of the automated voltage switcher.

trogen in the laser-ablation zone, and hence, form the cyano radicals *in situ*. The nitrogen reactant acts as a seeding gas as well.

B. Automated voltage switcher box

The carbon rod was mechanically attached to a linear position transducer. In our setup we used the 2 in. MLT model from Data Instruments. The transducer is basically a potentiometer with a resistance of 1500 Ω per inch of travel length. The +15 V supply is applied to the transducer through two 3.3 V Zener diodes (1N746), cf. Fig. 1. The output of the transducer goes from 3.3 to 11.7 V as an indication of the linear position. This signal is buffered by U1 and fed into two comparators (U2 and U3), which detect the high and low limit of the travel. These limits are set by two ten-turn potentiometers (VR1 and VR2). The outputs of both comparators are fed into a set/reset flip-flop (4027) to control the reversing of travel for the carbon rod. Outputs of the flip-flops are buffered and drive the bridge drivers consisting of two RFP10P15 and two NDP406BEL. The combination of three 1N914B, 10 k Ω resistors and the 1 μ F capacitor is to form a delay circuit to keep the output drivers from being both on during the transition period. The load in the circuit is the motor that drives the carbon rod and the motor power supply of 25 V and 0.5 A is external to the "automated voltage switcher box." This integrated feedback system maintains a constant speed in either direction, necessary for a

high long-term stability and reproducibility for laser-ablation processes and the generation of CN radicals.

C. Data acquisition of the pulsed CN($X^2\Sigma^+$) beam

Time-of-flight spectra of the supersonic beam were monitored on axis using a triply differentially pumped quadrupole mass spectrometer with electron-impact ionizer, rotatable in the plane of the beams with respect to the interaction region, and a Daly-type ion detector. The signal is amplified, converted to the transistor-transistor logic (TTL) standard, and fed into two multichannel scalers I (MCS I; laser "on" signal) and II (MCS, laser "off" signal) with a dwell time adjustable between 1 and 10 μ s. A four-slot chopper wheel located between the skimmer and the interaction region is attached to a three-phase motor (model 75A1004-2, Globe Motors) and spins at 240 Hz. The 960 Hz output of an infrared diode mounted at the top of the motor frame defines precisely the time zero of the experiment. If we choose different delay times between the initial photodiode pulse and the pulsed valve, distinct 9 μ s slices of the pulsed CN beam are selected. The frequency of this motor is controlled by a homebuilt, high-stability oscillator, cf. Sec. IID. The signal of the infrared diode is fed into a frequency divider to yield a 60 Hz trigger pulse. The pulsed valve of the primary source is triggered with delays between 918 and 940 μ s. If we perform reactive scattering experiments with the CN radical, a pulsed valve in the secondary source chamber opens between 10 and 50 μ s (depending on the reactant gas) prior to pulsed

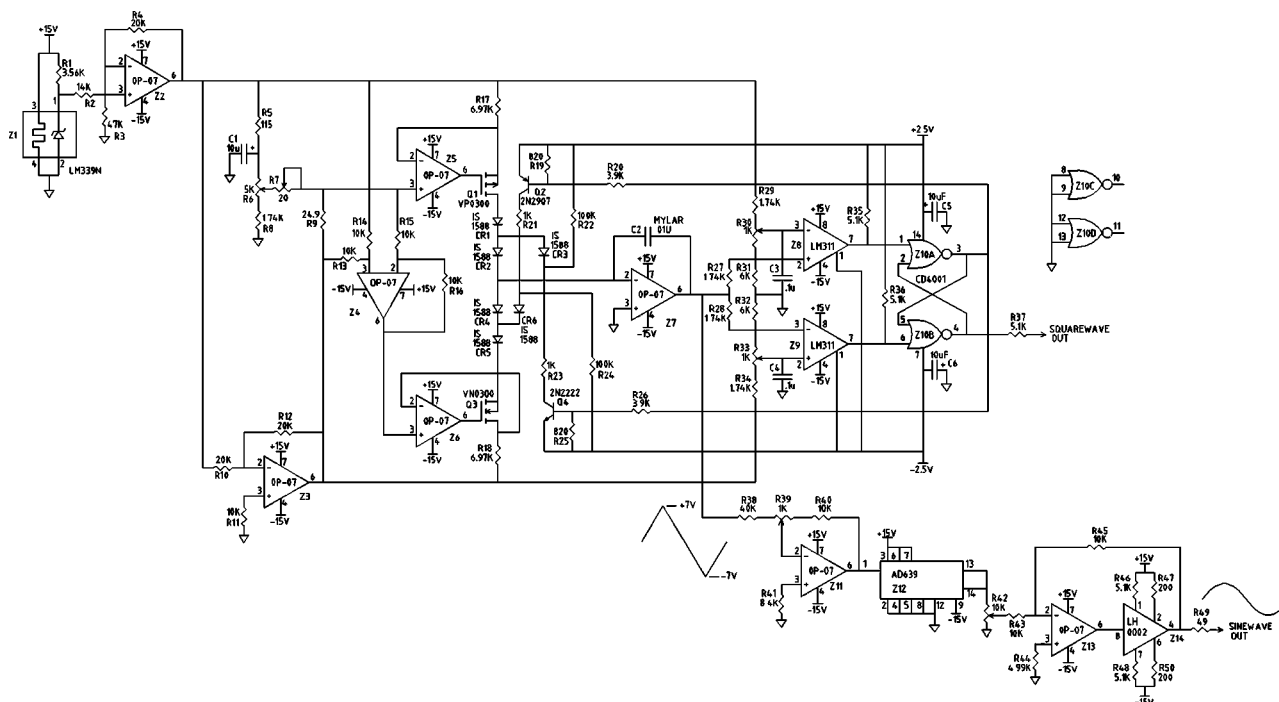


FIG. 2. Circuit diagram of the high-stability oscillator.

valve I. A second frequency divider divides the 60 Hz output by 2. This output triggers the flash lamps of the ablation laser 16603 μs and the Q-switch 16783 μs after the photodiode pulse. The present trigger sequence records time-of-flight spectra with “laser on” (MCS I) and “laser off” (MCS II) to enable pulsed valve modulated background subtraction.

D. High-stability analog oscillator

The laser chopper wheel driver had to be very stable and its frequency continuously adjustable, c.f. Fig. 2. First, we tested the IL 8038 Function Generation chip with a heat sink to keep the temperature constant. The results were very discouraging. The variations were in the order of 1%. Therefore, we decided to design a discrete circuit based on that chip. For the current switch, we chose a diode network instead of an active switch. The diodes are fast, clean, and simple to use. They do not have the problems associated with the bipolar transistor switches like the uncertain saturation voltages, nor the charge injection of the junction field-effect transistors. We used the IS1588 diodes. Their reverse-bias leakage current is one order of magnitude lower than the popular 1N914. All parts are readily available, except perhaps for the AD630 Universal Trigonometric Function Converter chip. The resistors are 1%, except for R10, R12, R13, R14, R15, and R16 that are 0.1%. The precision voltage reference is the oven-controlled LM339. The op-amps used are the precision OP-07. A buffer LH0002, capable of driving coax cables is placed at the sine-wave output. The comparator chose is the precision LM311.

The circuit works as follows. Z2 provides +10 V, by amplifying the 6.95 V reference of LM339. Z3 converts the +10 V into -10 V. R6 is the coarse frequency control. It is a ten-turn wire wound potentiometer. The fine adjustment is done by a single-turn composite R7. These potentiometers

provide the reference voltage for the constant current sources. Note this voltage is referred, respectively, to + and -10 V and not to ground. The positive current is generated by Z5, Q1, and R17. The negative by Z6, Q3, and R18. Z4 is a differential amplifier that changes the positive reference voltage into a corresponding negative one, referred to -10 V. Diodes CR1 and CR2 feed the positive current into the integrator Z7, while CR4 and CR5 sink the same current. These currents can be diverted by CR3 and CR4 when the transistors Q2 and Q4 are turned on, thus effectively shutting off the corresponding current sources. Z8, Z9, and Z10 form a precision Schmidt trigger that selects the correct sign current sources at any time. The output of the integrator Z7 is a continuous precise triangular wave form that goes from +7 to -7 V. This wave form is attenuated by Z11, because the input to AD639 has to be 1 V. Finally, Z13 and Z14 amplify the sine wave into the desired amplitude. This circuit yielded frequency stability of ± 100 ppm.

III. RESULTS

A. Velocity and speed ratio of the supersonic CN radical beam

Figure 3 displays typical TOF spectra of $m/e=26$ (CN^+) recorded at different delay times between the diode and the primary pulsed valve using an electron energy of 200 eV, 1700 V photomultiplier voltage and 25 kV applied to the Daly detector. The velocity v and speed ratio S of the cyanogen beam were determined by fitting the TOFs after time offset correction to

$$N(v) = v^2 \exp\left[-\left(\frac{v}{a} - S\right)^2\right], \quad (1)$$

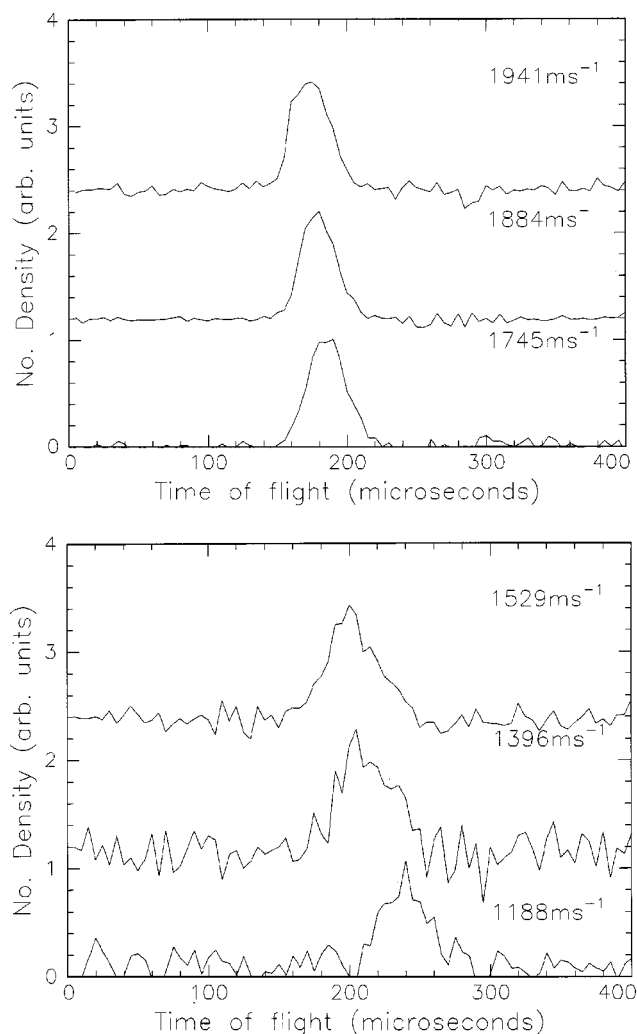


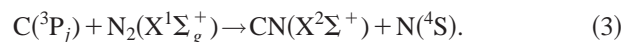
FIG. 3. Time-of-flight (TOF) spectrum of the $\text{CN}(X^2\Sigma^+)$ at distinct beam velocities after 2500 laser shots. The relative beam intensities are about 0.4, 1.0, 0.4, 0.24, 0.1, and 0.1 from 1941 down to 1188 ms^{-1} .

after convolution over the ionizer length and the shutter function of the chopper wheel with the number density of molecules with velocity v , $N(v)$, $a = m/2RT$, mass of the molecule m , the temperature of the beam T , and the ideal gas constant R . This procedure gives velocities of the seeded cyanogen beam between $v = 900 \text{ ms}^{-1}$ (delay diode-pulsed valve = $918 \mu\text{s}$) and 1920 ms^{-1} (delay diode-pulsed valve = $918 \mu\text{s}$), cf. Table I. Speed ratios range from $S = 8.0$ to 4.0 . Crossing these beams with a second, unsaturated hydrocarbon beam of acetylene, ethylene, allene, and/or methylacetylene gives collision energies tunable between 5.3 and 35.0 kJ mol^{-1} . Long-term fluctuations and day-to-day reproducibility of the CN beam velocity are, typically, within 3%. The high-stability oscillator and the automated voltage switcher are both crucial to this stability. Since the source is pulsed, a fluctuation in the oscillator period translates into variations of the chopper wheel rotation frequency, and hence, selecting a different part of the pulsed CN beam. In our experiments, we find that the variation of $\pm 0.1 \mu\text{s}$ at a period of $1041.67 \mu\text{s}$ is essential to ensure velocity fluctuations of less than 3%. Due to the automated voltage switcher box, the graphite rods are ablated more homogeneously than

in the previous design,¹⁶ and the carbon rod has to be replaced only once after about 5×10^7 laser shots.

B. Composition of the beam

Our on-axis characterization indicates that the beam contains small amounts of CN_2 isomers ($m/e = 40$).¹⁷ If we account for different ionization cross sections, relative intensities of $[\text{CN}]/[\text{CN}_2] = 1000\text{--}2000$ are derived. We like to stress that no higher carbon-nitrogen species such as C_2N , C_2N_2 , C_2N_3 , C_3N , C_3N_2 , C_3N_3 , etc. could be sampled in our supersonic beam within the detection limits of our system. Besides CN and CN_2 , the beam shows contribution of $\text{C}(^3\text{P}_j)$, C_2 , and C_3 as well. The presence of C_3 does not interfere in our experiments, since C_3 clusters were found not to react with unsaturated hydrocarbons if the collision energy in the crossed beams experiment is below 45.0 kJ mol^{-1} .¹⁸ Further, the concentration of $[\text{CN}]$ vs $[\text{C}_2]$ is about 10. These data together with reaction rate constants one order of magnitude lower for the C_2 reactions documents and different chemical dynamics for both reactions that the contribution to the reactive scattering signal of C_2 is marginal. Further, the masses of CN ($m/e = 26$) and C_2 ($m/e = 24$) differ by 2 amu; if C_2 reacted, the parent mass of the reaction products would differ by 2 amu as well, and hence, no interference is expected. We like to point out that we have no definite conclusion for the mechanism to form CN radicals. However, a look at the thermochemistry of reactions (2) and (3) shows that both processes are endothermic, and hence, very likely proceeds in the ablation center where excess energy is available to compensate the reaction endothermicity. A chemical reaction of ground-state species can be ruled out:



C. Number density of CN radicals in the interaction region

To determine the number density of the CN radicals in the interaction region, we calibrated the mass spectrometer with a helium and neon beam of known intensity. In addition, we measured on axis the relative ratio of the number of densities of $\text{C}(^3\text{P}_j)$ to CN. After correcting for the fragmentation pattern of the higher carbon cluster, and applying the relation between the number density $n(r)$ at a distance r from the nozzle with diameter D and the number density n_0 in the gas reservoir, $n(r) = 0.15 \times n_0 (r/D)^{-2}$,¹⁹ we find number densities of about $2\text{--}3 \times 10^{11} \text{ CN radicals cm}^{-3}$ in the interaction region. Hence, this newly developed CN source is three orders of magnitude more intense than previous supersonic CN sources based on photodissociation of C_2N_2 at 193 nm .¹³

To demonstrate the performance of this source explicitly in crossed molecular beam experiments, we performed test reactions of the CN beam crossing pulsed beams of C_2H_2 ,²⁰ C_2H_4 , C_3H_4 , CH_3CCH ,²¹ and C_6H_6 . Reactive scattering signal originating from the CN vs H exchange channel was detected in all systems, cf. reactions (4)–(7). Figure 4 shows a typical TOF spectrum together with the most probable

Newton diagram of reaction (8) taken at $m/e = 102$ close to the center-of-mass angle of 52.8° [$v(\text{CN}) = 1720 \text{ ms}^{-1}$; $S(\text{CN}) = 4.6$; $v(\text{C}_6\text{H}_6) = 755 \text{ ms}^{-1}$; $S(\text{C}_6\text{H}_6) = 12.3$; collision energy $E_C = 34.4 \text{ kJ mol}^{-1}$]. Data were accumulated for 1 h:



D. Excited states and vibrational state distribution of the CN radicals

Although our universal detector cannot determine the electronic and vibrational state distribution of the CN radicals directly, it is possible to give a qualitative picture of the internal state distribution. If we chose the velocity of the CN beam to be less than 1950 ms^{-1} , the experimentally derived reaction exothermicities of crossed beam reactions (4)–(8) are in excellent agreement with thermochemical data and recent *ab initio* calculations.^{20,21} Higher velocities of the pulsed CN beam are available as well, but the experimentally derived reaction exothermicities are too high in our crossed-beam reactions. Test experiments of reactions (4)–(6) selecting $v(\text{CN}) = 1980, 2279, 2308,$ and 2540 ms^{-1} , i.e., picking the faster parts of the pulsed CN beam, show that an excess energy of about 30–60, 50–80, 60–100, and 100–150 kJ mol^{-1} , respectively, is necessary to fit our experimental data. This suggests that at CN beam velocities $>1920 \text{ ms}^{-1}$ the CN radicals are either electronically or vibrationally excited. All electronically excited states of the CN radicals have lifetimes in the ns regime; only the $A^2\Pi$ state, which lies $109.1 \text{ kJ mol}^{-1}$ above the electronic ground state, holds a lifetime of about $7.0 \pm 0.5 \mu\text{s}$.²² Based on the energetics, this order of magnitude could account for the deviations at very high CN beam velocities; since, however, the CN radicals have a flight time of at least $8 \mu\text{s}$ at 2540 ms^{-1} from the ablation zone to the interaction region, electronically excited CN radicals can be likely ruled out. On the other side, the $\text{C}\equiv\text{N}$ stretching mode needs 24.8 kJ mol^{-1} to be excited. Therefore, our data suggest that as the velocity of the CN beam exceeds 1920 ms^{-1} , higher vibrational states of the CN radical are populated as well. As the velocity increases, the number density of the seeding N_2 molecules decreases in the pulsed supersonic expansion, and hence, the collision-induced quenching of the vibrationally excited CN radical is expected to decrease. This is in line with an enhanced energy excess corresponding to an increasing vibrational excitation of the CN radicals as the velocity increases. At our highest velocities, vibrational levels u to $\nu = 4-6$ might be populated.

IV. DISCUSSION

The *in situ* generation of a supersonic $\text{CN}(X^2\Sigma^+)$ beam via laser ablation of graphite and reaction of the ablated species with the N_2 carrier gas yields a high-intensity ($2-3$

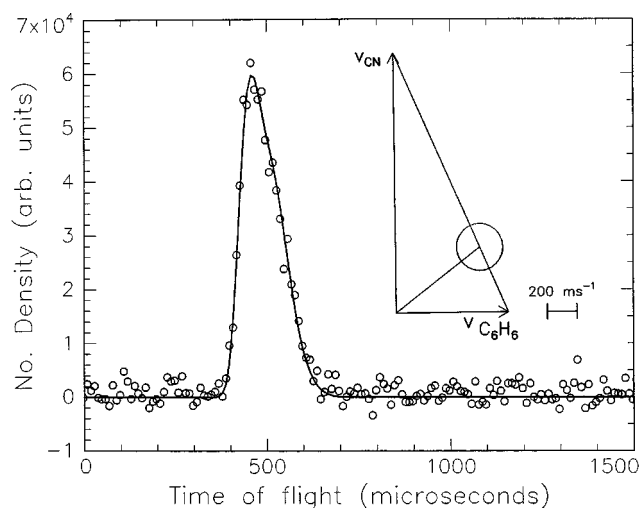


FIG. 4. Time-of-flight (TOF) spectrum of reactive scattering signal of the reaction $\text{CN}(X^2\Sigma^+) + \text{C}_6\text{H}_6 \rightarrow \text{C}_6\text{H}_5 + \text{CN} + \text{H}$ at the center-of-mass angle (dots indicate the experimental data, the solid lines the calculated fit) together with the most probable Newton diagram. The circle stands for the maximum center-of-mass recoil velocity of the product assuming all available energy channels into the translational degrees of freedom.

$\times 10^{11} \text{ CN radicals cm}^{-3}$) pulsed radical beam employable in crossed molecular beam experiments. Compared to other currently operating supersonic CN sources, the intensity of our newly developed source is up to three orders of magnitude higher, thus allowing us to study the chemical dynamics of crossed molecular beam reactions of CN radicals with a great variety of reactant molecules which was impossible before, c.f. Sec. III C. Second, the continuously tunable velocity regime extends from 900 to 1920 ms^{-1} giving collision energies with neat unsaturated hydrocarbons between 5.3 and 35.0 kJ mol^{-1} . Therefore, the collision energy-dependent chemical dynamics of CN crossed-beam reactions can be investigated as well. Third, the CN source is extremely stable; the high-stability analog oscillator driving the motor of the chopper wheel together with a high-precision reversible motor driver interfaced to the rotating carbon rod, are both essential to generate a stable cyanogen radical beam with velocity fluctuations of less than 3%. Currently, reproducible beam characteristics are accomplished ablating single carbon rods up to 500–600 h. These advantages make this source an extremely versatile source of highly unstable, and hence, very reactive diatomic radicals. In future studies, the carbon rod can be replaced by a boron or silicon rod. If we use N_2 , CO , CS , or O_2 as a seeding/reactant gas, we should be able to generate supersonic beams of BC , BN , BO , BS , CS , SiC , SiN , SiO , and SiS , which are expected to play a crucial role in interstellar chemistry, chemistry in the solar system, and/or combustion processes. This potential clearly shows the universal nature of this source to form a supersonic beam of otherwise highly refractive species, especially SiC and BN , *in situ*—an approach which will boost the investigation of the chemical reaction dynamics of reactions involving extremely reactive species which are very difficult to produce otherwise.

ACKNOWLEDGMENTS

One of the authors (R.I.K.) is indebted to the Deutsche Forschungsgemeinschaft (DFG) for a Habilitation fellowship (HC1-Ka1081/3-1) and Professor D. Gerlich (Technical University Chemnitz, Germany) for support. The work was further supported by Academia Sinica and the Taiwanese Petroleum Corporation. The work in Berkeley was supported by the U.S. Department of Energy.

¹D. W. Clarke and J. P. Ferris, *Origins of Life and Evolution of the Biosphere* 27, 225 (1997).

²B. Letourneur and A. Coustenis, *Planet. Space Sci.* **41**, 393 (1993).

³D. W. Clarke and J. P. Ferris, *Icarus* **115**, 119 (1995); **115**, 119 (1995).

⁴I. Cherchneff and A. E. Glassgold, *Ap. J.* **419**, L41 (1993).

⁵I. Cherchneff and A. E. Glassgold, *Ap. J.* **419**, L41 (1993); T. J. Millar and E. Herbst, *Astron. Astrophys.* **288**, 561 (1994); S. D. Doty and C. M. Leung, *Ap. J.* **502**, 898 (1998); I. Cherchneff, A. E. Glassgold, and G. A. Mamon, *ibid.* **410**, 188 (1993).

⁶*Reactive Intermediates in the Gas Phase*, edited by D. W. Setser (Academic, New York, 1979); *Reactive Intermediates*, edited by R. A. Abramovich (Plenum, New York, 1980); *Short-Lived Molecules*, edited by M. J. Almond (Ellis Horwood, New York, 1990); I. W. M. Smith, in *The Chemical Dynamics and Kinetics of Small Molecules*, edited by K. Liu and A. Wagner (World Scientific, Singapore, 1995), p. 214.

⁷D. L. Yang and M. C. Lin, in *The Chemical Dynamics and Kinetics of Small Molecules*, edited by K. Liu and A. Wagner (World Scientific, Singapore, 1995); p. 164, and references therein.

⁸I. R. Sims *et al.*, *Chem. Phys. Lett.* **211**, 461 (1993); I. W. M. Smith, I. R. Sims, and B. R. Rowe, *Chem.-Eur. J.* **3**, 1925 (1997).

⁹G. Scoles, *Atomic and Molecular Beam Methods* (Oxford University Press, New York, 1988), Vol. 1.

¹⁰Y. T. Lee, *Science* **236**, 793 (1987).

¹¹J.-H. Wang, K. Liu, G. C. Schatz, and M. Ter Horst, *J. Chem. Phys.* **107**, 7869 (1997); L.-H. Lai, J.-H. Wang, D.-C. Che, and K. Liu, *ibid.* **105**, 3332 (1996); D.-C. Chil, K. Liu, *Chem. Phys. Lett.* **243**, 290 (1995); D.-C. Liu, *Chem. Phys.* **207**, 367 (1996).

¹²R. G. MacDonald *et al.*, *Can. J. Chem.* **72**, 660 (1993); D. M. Sonnenfroh, R. G. MacDonald, and K. Liu, *J. Chem. Phys.*, 1478 (1990).

¹³K. Liu (unpublished).

¹⁴W. Sun, R. I. Kaiser, and Y. T. Lee (unpublished).

¹⁵D. Proch and T. Trickl, *Rev. Sci. Instrum.* **60**, 713 (1989).

¹⁶R. I. Kaiser, Y. T. Lee, and A. G. Suits, *J. Chem. Phys.* **103**, 10395 (1995).

¹⁷Three CN₂ isomers exist, i.e., NCN($X^3\Sigma_g^-$); CNN($X^3\Sigma^-$); and *c*-CN₂(X^1A_1); G. Herzberg, *Molecular Spectra and Molecular Structure* (1991), Vol. 3; J. M. L. Martin *et al.*, *Chem. Phys. Lett.* **226**, 47 (1994).

¹⁸N. Balucani, Y. T. Lee, and R. I. Kaiser (unpublished).

¹⁹P. C. Engelking, *Chem. Rev.* **91**, 399 (1991).

²⁰L. C. L. Huang, Y. T. Lee, and R. I. Kaiser, *J. Chem. Phys.* **110**, 7119 (1999).

²¹L. C. L. Huang, Y. Osamura, N. Balucani, Y. T. Lee, and R. I. Kaiser, *J. Chem. Phys.* **111**, 2857 (1999).

²²H. Okabe, *Photochemistry of Small Molecules* (Wiley, New York, 1978).